Investigation of Ammonium- and Phosphonium-Based Deep Eutectic Solvents as Electrolytes for a Non-Aqueous All-Vanadium Redox Cell

L. Bahadori,[a] M. A. Hashim,[a] N. S. A. Manan,[b] F. S. Mjalli,[c] I. M. AlNashef,[d] N. P. Brandon,[e] and M. H. Chakrabarti[e,*,z]

[a]*Department of Chemical Engineering, Faculty of Engineering, University of Malaya, Kuala Lumpur-50603, Malaysia*
[b]*Department of Chemistry, Faculty of Science, University of Malaya, Kuala Lumpur-50603, Malaysia*
[c]*Petroleum & Chemical Engineering Department, Sultan Qaboos University, Muscat 123, Oman*
[d]*Department of Chemical and Environmental Engineering, Masdar Institute of Science and Technology, Abu Dhabi, United Arab Emirates*
[e]*Department of Earth Science and Engineering, Imperial College London, South Kensington, London SW7 2AZ, United Kingdom*

The charge/discharge characteristics for vanadium acetylacetonate in deep eutectic solvents were evaluated using an H-cell with an anion-exchange membrane separator for the first time. Coulombic (CE) and energy efficiencies (EE) of the electrolyte containing $V(acac)_3$/0.5 M $TEABF_4$ in DES3 (a hydrogen bonded eutectic between choline chloride and ethylene glycol) were obtained as 49–52% and 25–31%, respectively, when charging from 0 to 50% of theoretical maximum state-of-charge for 12 cycles. The low CE may be due to the crossover of the active species through the separator, or to the loss of active vanadium due to a parasitic reaction. However, the CE was similar to that for acetonitrile (CH_3CN) indicating the promise of DESs as suitable electrolytes for future evaluation. Charge and discharge voltages are respectively higher and lower than the formal cell potential obtained by voltammetry. Ohmic drop in the DES results from the low conductivity of the electrolyte and the relatively large distance between the two electrodes in the H-cell. Further studies require investigation in a flow cell with analyses of polarization curves and impedance to determine the loss mechanisms in sufficient detail.

Manuscript submitted August 14, 2015; revised manuscript received January 7, 2016. Published January 20, 2016.

Low energy density is often reported as a barrier in the commercialization of redox flow batteries using current aqueous electrolytes.[1] Non-aqueous electrolytic solvents offer a wide potential window of operation and increase the energy capacity of the system.[2–4] In contrast to organic systems which are either scarce or environmentally unfriendly, ionic liquids (ILs) have emerged as a relatively new class of non-aqueous electrolytes for energy storage applications.[5–9] ILs are salts that are liquid below 100°C. ILs have many favorable characteristics, e.g., low volatility, high intrinsic conductivity, large electrochemical window, etc. In addition, ILs can be tuned by combining different cations and anions. However, many reports point out the hazardous toxicity and the poor biodegradability of most ILs.[7] ILs with high purity are also required since impurities, even in trace amounts, affect their physical properties. Additionally, their synthesis is not entirely environmentally friendly since it generally requires a large amount of salts and solvents in order to completely exchange the anions.[10] These drawbacks together with the high price of common ILs unfortunately hamper their industrial applications. Such issues may be overcome by using deep eutectic solvents (DESs).[11,12]

A DES is a eutectic mixture of an organic salt (ammonium or phosphonium) and a hydrogen bond donor (HBD), that is made up of different components such as amides, metallic salts, alcohols, carboxylic acids and amines that may be used as complexing agents (typically an H-bond donor).[13,14] DESs have a melting point that is far below that of either individual constituent. The mechanism is that the complexing agent interacts with the anion and increases its effective size. This, in turn, decreases the anionic interaction with the cation thereby reducing the salt-HBD lattice energy and causing a depression in the melting point of the mixture.[15] These liquids are easy to prepare in a pure state, they are non-reactive with water and most importantly they are biodegradable, and hence the toxicological properties of the components are well characterized.[16] These compounds share many characteristics of conventional ILs (e.g., they have intrinsic electrical conductivity, low-volatility, biodegradability, high thermal and chemical stability, good electrochemical stability, and non-flammability) and they are simple to synthesize on a large scale.[17–19] These properties have been explored in promising applications such as solvents for electrodeposition and electropolishing,[20,21] electrochemistry,[10] separation processes,[22] chemical and enzymatic reactions,[23] biochemistry[24] as well as organic and inorganic synthesis.[25,26]

Several DESs were prepared based on quaternary ammonium and phosphonium salts and different hydrogen bond donors (HBDs).[27] Furthermore, their physicochemical and electrochemical properties (viscosity, conductivity, electrochemical stability, diffusion coefficients, etc.) have been evaluated in a similar manner to that for ILs. The synthesized DESs are applied as electrolytes to determine the effects of the electrode and solvent in our electrochemical system. Ferrocene/ferrocenium (Fc/Fc^+) or cobaltocenium/cobaltocene (Cc^+/Cc) redox couples have been investigated as candidates of internal references to provide a known and stable reference point in various DESs.

Despite the significance of DESs and their remarkable advantages, their applications in redox flow batteries (RFBs) are limited.[28] In this work we describe a single-element non-aqueous redox system based on vanadium (III) acetylacetonate [$V(acac)_3$] in selected DESs. The potential application of DESs in non-aqueous RFBs was evaluated using cyclic voltammetry and charge–discharge characteristics. The latter was estimated using a static H-type electrochemical glass cell reactor with a commercial anion-exchange membrane.

The experiments reported here are based on commercially sourced raw materials without additional purification (i.e., these are preliminary experiments that enable an informed decision for choosing appropriate raw materials for preparing DESs for practical experiments with non-aqueous RFB prototypes in future work). The purpose is to prove that a redox battery could be charged/discharged successfully without the need for complex synthesis and purification processes that could possibly lower the economics of the entire process.

Experimental

Materials.—Choline chloride (ChCl) ($C_5H_{14}ClNO$), methyltriphenylphosphonium bromide ($C_{19}H_{18}PBr$), N,N-diethylenethanol ammonium chloride ($C_6H_{16}ClNO$), glycerin ($C_3H_8O_3$), ethylene glycol ($C_2H_6O_2$), triethylene glycol ($C_6H_{14}O_4$), malonic

*Electrochemical Society Member.
[z]E-mail: m.chakrabarti@imperial.ac.uk

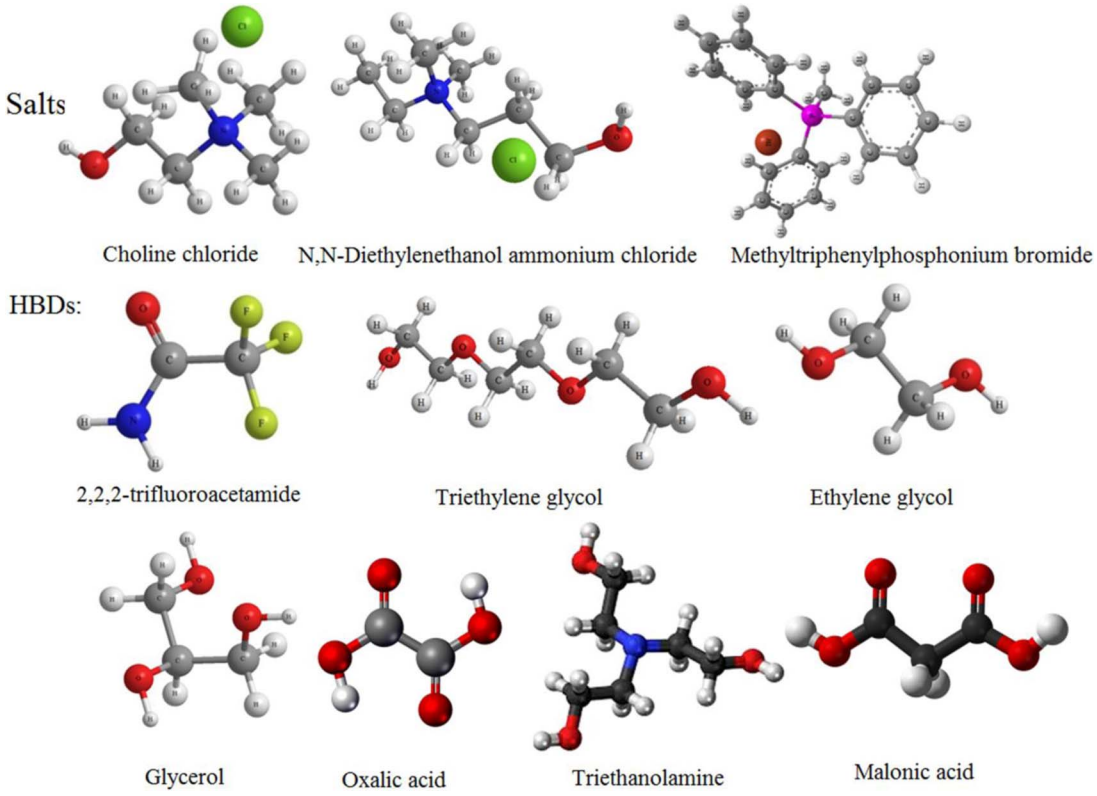

Figure 1. Structures of salts include bulky cations and smaller anions attached to HBDs. Some portions of this figure are similar to our earlier publications.[11,12]

acid ($CH_2(COOH)_2$), oxalic acid (HOOC-COOH), triethanolamine ($N(CH_2CH_2OH)_3$) and 2,2,2-trifluoroacetamide (F_3C-CO-NH_2), were purchased from Merck Chemicals (Germany) with purity of more than 98%. Moreover, the water mass fraction in these commercially sourced chemicals, as per the manufacturer's guide, was less than 10^{-4}%. All chemicals were used as received in an inert glove box (Innovative Technology, Pure Lab^{HE}, USA) purged with argon (oxygen and moisture free) at all times. At no time were these chemicals exposed to the atmosphere.

Preparation of DESs.—The original procedure of synthesizing DESs as reported by Abbott et al.[29] and Mjalli et al.[30] was used in this work. Briefly, a jacketed cup with a magnetic stirrer was used to mix both the salt and HBD at 383.15 K (at a maximum) and atmospheric pressure for a period of 3 h (at a minimum) until a homogenous colorless liquid was formed. The synthesis experiments were conducted in the glove box with firm humidity control of less than 4 ppm water. Figure 1 shows the structures of the salts and hydrogen bond donors that make up the DESs chosen for this study and Table I presents the compositions of the different DESs synthesized for this investigation.

Electrochemical cell.—The electrochemical cell consisted of a typical three-electrode set-up. The counter electrode was a Pt wire, and an Ag wire (immersed in 65% HNO_3 prior to experiments, then rinsed thoroughly with water and ethanol) was used as a quasi-reference electrode (QRE).[27,30] Glassy Carbon (GC, 3 mm diameter) was used as the working electrode. The working electode was carefully polished before each voltammetry experiment with 0.3 μm alumina paste (Wirth Buehler) and ultrasonically rinsed in acetone. The electrochemical cell was assembled within a Faraday cage, which in turn was situated inside the dry argon-filled glove box.

Table I. List of DESs obtained by complexation between hydrogen acceptor and hydrogen-bond donor molecules used in this study.

Hydrogen acceptor (Salts)	Hydrogen-bond donor	Molar ratio (salt : HBD)	Abbreviation
Choline chloride	Triethylene glycol	1:3	DES1
Choline chloride	Glycerol	1:2	DES2
Choline chloride	Ethylene glycol	1:2	DES3
Choline chloride	Malonic acid	1:1	DES4
Choline chloride	Oxalic acid	1:1	DES5
Choline chloride	Triethanolamine	1:2	DES6
Choline chloride	2,2,2-Trifluoroacetamide	1:2	DES7
N,N-Dimethylmethyleneiminium chloride	Triethylene glycol	1:3	DES8
N,N-Dimethylmethyleneiminium chloride	Glycerol	1:2	DES9
N,N-Dimethylmethyleneiminium chloride	Ethylene glycol	1:2	DES10
N,N-Dimethylmethyleneiminium chloride	Malonic acid	1:1	DES11
Methyltriphenylphosphonium bromide	Triethylene glycol	1:4	DES12
Methyltriphenylphosphonium bromide	Glycerol	1:3	DES13
Methyltriphenylphosphonium bromide	Ethylene glycol	1:2	DES14

Cyclic Voltammetric measurements.—All electrochemical experiments were performed using a computer-controlled Autolab PGSTAT302N potentiostat/galvanostat (Ecochemie, Netherlands) with Nova software. The electrochemical behavior of the system was obtained by performing a series of different potential steps and recording the current-time response curves. The potential was varied linearly at scan rates (ν) from 10 to 1000 mVs^{-1}.

Solubility of vanadium acetylacetonate in DESs.—The solute was added to the solvent and the mixture agitated for >24 h. This was repeated until undissolved solute was observed.

Samples from the solution were then taken, filtered and analyzed using a Perkin-Elmer Optima 5300DV inductively coupled plasma-atomic 69 emission spectrometer (ICP-AES). Each analysis was repeated at least three times and the average taken.

H-type cell charge/discharge.—An H-type glass cell was designed and fabricated for the constant current charge and discharge tests of a small redox battery with vanadium redox couples. This H-type glass cell consists of three principal parts, the anodic and cathodic compartments and the membrane placed in between. The H-type cell is commonly utilized to screen electrolytes for prototype RFB experiments.[3,31,32]

6 mm diameter graphite rod electrodes were utilized as both anode and cathode for the charge–discharge of the H-type cell. The distance between the two electrodes in the H-type cell was 9 mm. Acetonitrile (anhydrous grade) was used as a standard for comparing the performance of the $V(acac)_3$ system with that of different DESs. Tetraethylammonium tetrafluoroborate ($TEABF_4$) was used as the supporting electrolyte to improve conductivity of the solvents. Each compartment contained about 15 ml of electrolyte with a magnetic stirrer.

An AMI-7001S anion exchange membrane (Membranes International Ltd., U.S.A.) was utilized in the H-type cell. The membrane was situated between two O-shaped silicon rubber gaskets and sealed to each gasket with silicon sealant in order to avoid any leakage. Expansion of AMI-7001S membrane from dry (as-shipped) to wet conditions was insignificant.

Charge–discharge tests are performed in an H-type glass cell using the galvanostatic method. The galvanostat used is an Autolab PGSTAT302N potentiostat/galvanostat (Ecochemie, Netherlands). All experiments have been performed at room temperature.

Results and Discussion

Electrochemical potential windows of DESs.—The limiting reduction and oxidation potentials of the DESs are analyzed by performing cyclic voltammetry using a GC working electrode at ambient temperature and a scan rate of 0.1 V s^{-1} as shown in Figure 2 (full details are available in our earlier publications[27,30,33] where the limiting current density reached 0.2 mA cm^{-2}). It is discovered that some of the tested DESs have similar potential ranges to typical ILs.[34] However, some ILs have wider electrochemical windows.[35,36] The screened potential windows (PWs) when compared with the electrochemical stability of $V(acac)_3$ show that redox couples can be observed within the stability window.

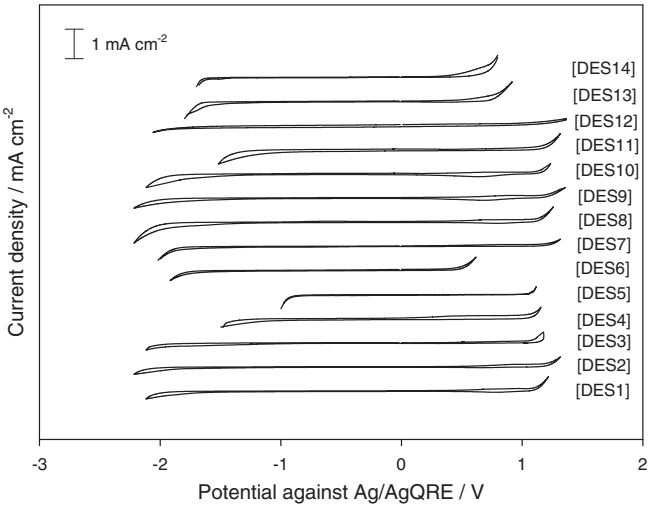

Figure 2. PWs of DESs based on ammonium and phosphonium salts and different HBDs. Experiments were performed using cyclic voltammetry with a glassy carbon working electrode at a scan rate of 0.1 V s^{-1}. Similar results are reported in our earlier publications and reproduced with permission from RSC, Elsevier and ECS respectively.[27,30]

Solubility of $V(acac)_3$ in DESs.—The solubility results for DES3, DES8 and DES10 are shown in Table II. These DESs are potential candidates as electrolytes to replace acetonitrile as a solvent for vanadium acetylacetonate [$V(acac)_3$]-based redox batteries.[31]

Cyclic Voltammetry of $V(acac)_3$ in DESs.—Figure 3 shows the voltammograms of 0.01 M $V(acac)_3$ in the four different DESs at a scan rate of 0.1 V s^{-1}. The results clearly show that DESs 3, 9 and 11 have potential for further evaluation and their standard open circuit cell potentials are listed in Table II. Results for other DESs are not shown here as our earlier experiments with ferrocene and cobaltocenium (Nernstian redox systems) couples displayed irreversible behavior.[11,12,27,30,33]

These current peaks are attributed to the redox couples observed in Figure 3 to the following eactions (as represented in Figure A1 of the Appendix for acetonitrile):

$$R_1/O_1: \quad V(III)(acac)_3 + e^- \Leftrightarrow \quad [V(II)(acac)_3]^- \qquad [1]$$

$$R_2/O_2: \quad V(III)(acac)_3 \quad [V(IV)(acac)_3]^- + e^- \qquad [2]$$

Figure 3 shows the cyclic voltammograms for the electrolyte containing 0.01 M $V(acac)_3$ and 0.5 M $TEABF_4$ in DES3, DES8, DES10 and DES14. Figure 4 compares different DESs at various scan rates in which, for the V(II)/V(III) redox couple in DES3, ΔE_p increased

Table II. Summary of $V(acac)_3$ electrochemical performance characteristics in selected DESs.

Electrolyte	Cell Potential (V)	$D \times 10^{-6}$ (cm^2 s^{-1})	$k^0 \times 10^{-3}$ [a] (cm s^{-1})		Solubility (M)
			V(II)/V(III)	V(III)/V(IV)	
CH_3CN[b]	2.18	3.50 (±0.06)	1.25(±0.08)	1.18(±0.07)	0.63(±0.05)
DES3	2.01	0.69 (±0.03)	0.74(±0.05)	1.02(±0.08)	0.25(±0.06)
DES8	1.98	0.02–0.13 (±0.05)	0.12(±0.07)	0.32(±0.02)	0.12(±0.04)
DES10[c]	2.01	0.59–0.63 (±0.08)	0.53(±0.04)	0.85(±0.03)	0.19(±0.07)

[a]Electrode rate constant for the vanadium acetylacetonate redox reaction
[b]Acetonitrile data is obtained from a separate publication[31]
[c]Other DESs are not shown as their cyclic voltammograms do not display any kind of reversible or quasi-reversible behavior

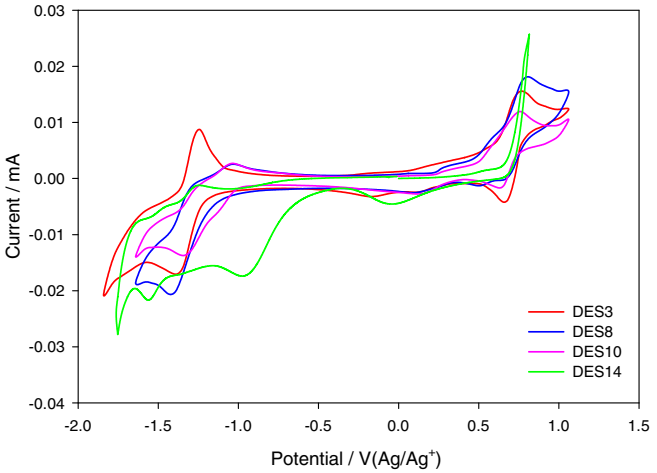

Figure 3. Cyclic voltammograms recorded at 0.1 V s^{-1} at a glassy carbon electrode in 0.01 M $V(acac)_3$ and 0.5 M $TEABF_4$ in DES3, DES8, DES10 and DES14.

from 60 to 90 mV and the ratio of anodic to cathodic peak currents increased from 0.97 to 1.20 as the scan rate was raised from 0.05 to 0.50 V s^{-1}. For the V(III)/V(IV) redox couple, ΔE_p increased from 65 to 80 mV but the ratio of anodic to cathodic peak currents decreased from 1.1 to 0.98 as the scan rate increased in DES3. The ratio of anodic to cathodic peak currents is close to unity.

For the V(II)/V(III) redox couple, ΔE_p increased from 80–116 mV and 92–135 mV for DES10 and DES8 respectively. The ratio of anodic to cathodic peak currents increased from 0.33–0.54 (for DES10) and 0.25–0.51 (for DES8) as the scan rate increased from 0.01 to 0.50 V s^{-1} (Figure 4). For the V(III)/V(IV) redox couple, ΔE_p increased from 85–122 mV (for DES10) and 90–145 mV (for DES8) but the ratio of anodic to cathodic peak currents decreased from 0.92–0.55 (for DES10) and 0.85–0.49 (for DES8) as the scan rate increased. From Figure 4, it can be deduced that both Reactions 1 and 2 are quasi-reversible in DESs 9 and 11.

The standard open circuit cell potential can be used to determine the potential of the system when no current is flowing through it via the Nernst equation (supposing the reactants and products of redox reactions behave relatively ideally, so that activity coefficients are unity):

$$E = E^0 - \frac{RT}{nF} \ln\left(\frac{[\text{products}]}{[\text{reactants}]}\right) \qquad [3]$$

where E is the measured potential, E^0 is the cell potential measured from cyclic voltammetry, R is the universal gas constant, T is the absolute temperature, n is the number of electrons, and F is Faraday's constant. For a single-electron disproportionation of a neutral intermediate active species, the product and reactant concentrations can be related to the total concentration of V, $[c]_{total}$, and the fractional state of charge (SOC), x, through:

$$[\text{Products}] = [c]_{total}x \qquad [\text{Reactants}] = [c]_{total}(1-x) \qquad [4]$$

Figure 5 indicates a plot of the cell potential as a function of the percentage state of charge (%SOC = 100 × SOC) in DES3, using the cell potential from Table II along with the condition that $V(acac)_3$ undergoes a single-electron disproportionation. The cell potential increases dramatically when the first 8% of the V(III) is converted to V(II) and V(IV) showing the expected logarithmic behavior. Then it increases slowly and passes through the equilibrium potential when half of the V(III) has reacted. When the solution is completely converted, the potential again increases dramatically toward infinity at 100% conversion (as predicted by the Nernst equation). This dramatic increase is indicative of overcharging as the Nernst equation does not hold at 100% conversion of the reactants.

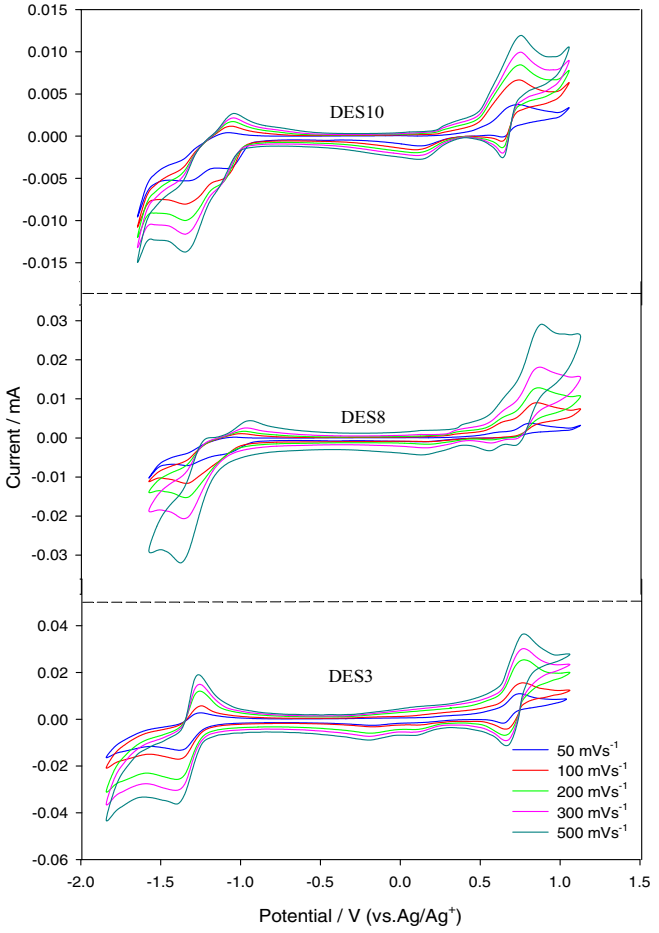

Figure 4. Cyclic voltammograms for 0.01 M $V(acac)_3$/0.5 M $TEABF_4$ in DES3, DES10 and DES8 using a glassy carbon electrode at a range of scan rates.

Variable-temperature studies of V(acac)$_3$ in DESs.—The low vapor pressures presented by DESs facilitates the recording of temperature dependence electrochemistry in the three-electrode cell over a temperature range of 298–328 K. Table III displays the results when the temperature was adjusted for the electrolyte. Anodic peaks were recorded at around 0.8, 0.6 and 0.7 V in DES3, DES8 and DES10, respectively, at 298 K for the positive cell, coinciding with the oxidation reaction of V(III) to V(IV). Cathodic peaks were observed at 0.72,

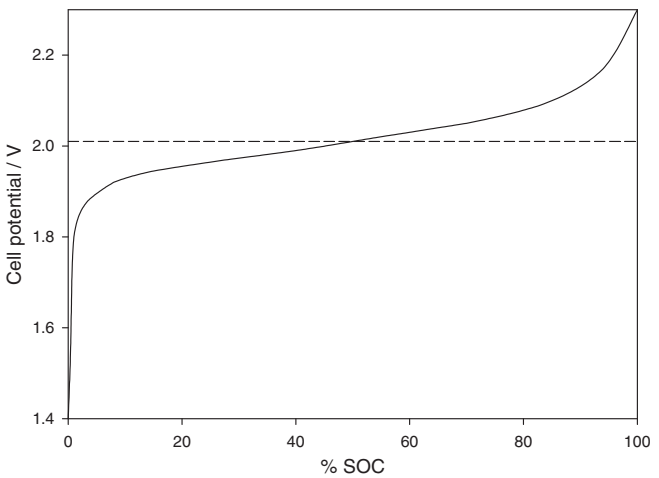

Figure 5. Plot of the Nernst equation for a single-electron disproportionation reaction with a 2.01 V cell potential (DES3).

Table III. Voltammetric data values of V(acac)$_3$ from CV result at different temperatures at a scan rate of 100 mVs^{-1} in selected DESs.

DESs	Temperature (K)	I_{pa} (mACm^{-2})	I_{pc} (mACm^{-2})	ΔE (mV)
DES3	Oxidation of V(III)/V(IV)			
	298	0.14	0.07	74
	308	0.19	0.09	66
	318	0.31	0.13	50
	328	0.35	0.20	42
	reduction of V(II)/V(III)			
	298	0.04	0.28	71
	308	0.06	0.32	65
	318	0.10	0.41	53
	328	0.13	0.49	48
DES8	Oxidation of V(III)/V(IV)			
	298	0.08	0.01	103
	308	0.16	0.03	91
	318	0.27	0.07	78
	328	0.33	0.11	56
	reduction of V(II)/V(III)			
	298	0.02	0.09	108
	308	0.08	0.17	92
	318	0.12	0.24	75
	328	0.15	0.33	62
DES10	Oxidation of V(III)/V(IV)			
	298	0.17	0.04	94
	308	0.25	0.07	85
	318	0.38	0.10	76
	328	0.49	0.15	58
	reduction of V(II)/V(III)			
	298	0.01	0.21	87
	308	0.04	0.35	77
	318	0.08	0.44	70
	328	0.10	0.52	61

0.5 and 0.6 V in DES3, DES8, and DES10, respectively, corresponding to the reduction reaction of V(VI) to V(III). I_{pa} and I_{pc} increased with temperature, implying an enhancement in the reaction rate. As the temperature increased, the ions moved faster and collided more frequently, and the proportion of collisions that can overcome the activation energy for the reaction increased with temperature. This is of particular relevance for the work with DESs due to its lower vapor pressures than acetonitrile thereby allowing significant data points to be collected at a range of temperatures. This is obviously not possible with acetonitrile.[2–4,31]

For the V(II)/V(III) redox couple at 298 K, anodic (1.25, −1.15 and −1.10 V) and cathodic peaks (−1.96, −1.258, −1.187 V) were observed in DES3, DES8, and DES10, respectively. With increasing temperature, the peak potential separation (ΔE) of both V(II)/V(III) and V(III)/V(VI) redox couples showed an obvious decrease, indicating that the redox reaction resulted in a better reversibility at higher operating temperatures.

The D of V(acac)$_3$ based on the cathodic peak currents for the V(III)/V(IV) redox couple are listed in Table II. The temperature dependence of diffusion coefficient can be examined with the Arrhenius equation (Eq. 5).

$$D = D_0 \exp\left(\frac{-E_D}{RT}\right) \quad [5]$$

Where D_0 is a constant corresponding to the hypothetical diffusion coefficient at infinite temperature, and E_D is the diffusional activation energy of the electroactive species. A plot of ln$D$ vs. 1/T can be obtained in Figure 6, which demonstrates a good correlation of the data to the Arrhenius relationship.

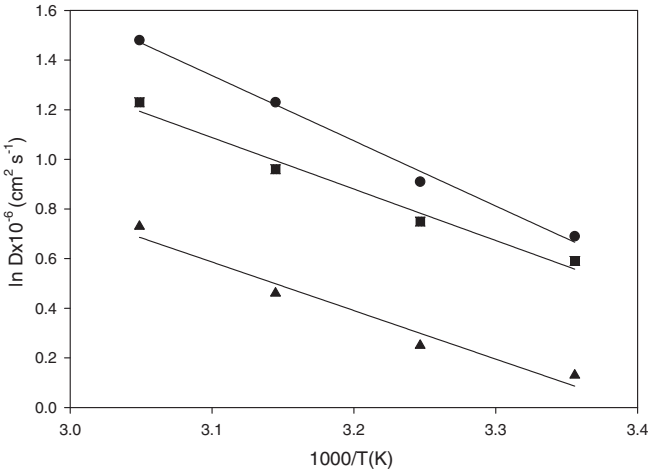

Figure 6. The plot of ln$D$ versus 1/T based on the cathodic peak currents for the V(III)/V(IV) redox couple on the GC electrode in DES3, DES8 and DES10.

Charge/discharge performance.—CH_3CN has been used to validate the results obtained with DES3. Galvanostatic charge and discharge has been performed with 0.01 M V(acac)$_3$ in CH_3CN consisting of 0.5 M $TEABF_4$ as reported above. The result is shown in Figure 7a for 2 cycles. The coulombic efficiency is nearly 50% at 50% SOC herein (similar to the results reported in the literature[31]), which confirms that the H-type glass cell reactor employed is worthy for investigation using DES3.

The charge/discharge cycle for the same electrolytes in DES3 was evaluated. Galvanostatic conditions were applied with potential cutoffs for both charge and discharge (Figure 7a). The charge cutoff was 2.40 V, being higher than the 2.01 V cell potential detected in the voltammetry for the one-electron disproportionation of V(acac)$_3$ in DES3. The discharge cutoff was set at 0 V to enable the system to completely discharge. Further charge/discharge cycling was performed and the electrolyte was found to be stable even after 10 cycles (Figure 7b).

As shown in Figure 7a, the charge voltage was as high as 2.40 V for the system, suggesting a total over potential of 400 mV with respect to the 2.01 V potential associated with the reaction. There was a small discharge voltage plateau in this system, around 0.5 V and 0.3 V for cycles 1–5 and cycles 6–12, respectively. The low discharge voltage may be due to the large ohmic drop and polarization in the H-type cell. Despite adding a supporting electrolyte, the ohmic drop was higher in the case of the DES. Ohmic overpotential was probably important due to the low conductivity of the electrolyte,[27] the relatively large distance between the two electrodes in the H-type cell, and the relatively low ionic conductivity of the membrane separator. The ohmic overpotential decreased the energy efficiency. The coulombic and energy efficiencies obtained had relatively constant values. Coulombic efficiency (CE) is the ratio of a cell's discharge capacity divided by its charge capacity, as described in Eq. 6.

$$CE = \frac{I_D t_D}{I_C t_C} \times 100\% \quad [6]$$

Where I_D and I_C are discharge and charge cell currents whereas t_D and t_C are discharge and charge times.

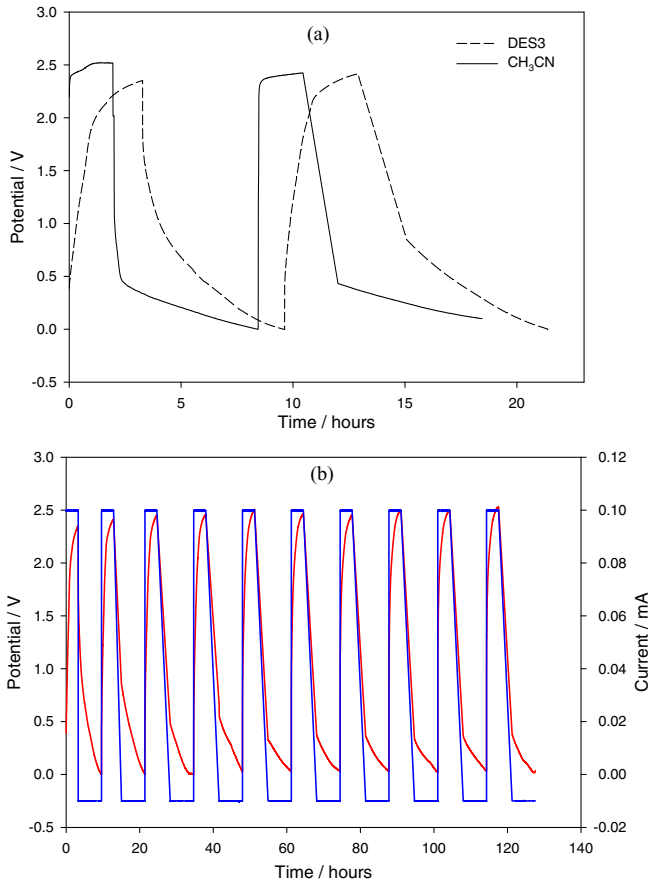

Figure 7. (a) Charge/discharge curves for (0.01 M $V(acac)_3$/0.5 M $TEABF_4$ in CH_3CN (the charge current was 1 mA and the discharge current was 0.1 mA) AND charge/discharge curves for 0.01 M $V(acac)_3$/0.5 M $TEABF_4$ in DES3 (the charge current was 0.1 mA and the discharge current was 0.01 mA); (b) Charge/discharge curves during the 3rd and 12th cycles for 0.01 M $V(acac)_3$/0.5 M $TEABF_4$ in DES3.

The CE for $TEABF_4$/ DES3 was 49.58% in cycle 1. It can be seen that the CE was similar to that for CH_3CN, showing the promise of DESs as potential electrolytes for future evaluation. The principal reason of low CE is likely to be due to the fact that the active materials are in solution. When these are oxidized or reduced at the electrode, some portion of the reacted materials will diffuse away from the electrode surface and thus will be unavailable for the subsequent reduction or oxidation reactions when the potentials are reversed. Thus, a low CE from CV data is an inherent feature of solution-based electrochemistry in a static cell. It is only when the active materials are fixed at the electrode (i.e., solid electrodes) or when convection is used to return the dissolved active materials in solution to the electrode surface (as is done in redox flow cells where the anolyte and catholyte are continuously pumped past the electrodes) that CE values approaching 100% are achievable. In addition the low CE may be influenced by side reactions and/or the possible crossover of the active species through the anion-exchange membrane.

Energy efficiency (EE) is estimated from voltage efficiency (VE) and CE, as depicted in Eq. 7. VE is defined as the ratio of the cell mean discharge voltage (V_D) divided by its mean charge voltage (V_C), as displayed in Eq. 8.

$$EE = CE \times VE \quad [7]$$

$$VE = \frac{V_D}{V_C} \times 100\% \quad [8]$$

The CE for cycles 1–12 ranged from 49–52% at 50% SOC. These low values may occur owing to crossover of the active species through the membrane. EE values of approximately 25–31% were achieved.

Conclusions

Throughout the present work, fourteen DESs were synthesized. The DESs were characterized and the selected DES3 (formed by means of hydrogen bonding between choline chloride and ethylene glycol) was chosen as the electrolyte for charge/discharge tests (based upon preliminary experimental results briefly explained below) using non-aqueous all-vanadium acetylacetonate redox couples.

Results from voltammetry show that the $V(acac)_3$ complex can be reduced to $[V(acac)_3]^-$ and oxidized to $[V(acac)_3]^+$ at a GC electrode. In addition, the cyclic voltammograms indicate that $TEABF_4$ is stable in $V(acac)_3$ and DES3, DES8 and DES10 electrolytes between a voltage range of −2.5 to +1.5 V. Both V(II)/V(III) and V(III)/V(IV) redox reactions are reversible in DES3, and quasi-reversible in DES8 and DES10. The D for the DESs lies in the range of 0.02–0.69 × 10^{-6} cm^2 s^{-1} at room temperature. $V(acac)_3$ has reversible electrochemistry in DES3, but a much higher solubility is required to compete with aqueous or even organic (especially acetonitrile) systems.

The charge/discharge characteristics for the all-vanadium system were evaluated using an H-cell with an anion-exchange membrane separator. Coulombic and energy efficiencies of the electrolyte containing $V(acac)_3$/0.5 M $TEABF_4$ in DES3 were determined to be 49–52% and 25–31% respectively, when charging from 0% to 50% of theoretical maximum SOC for the first 12 cycles. The low CE may be due to crossover of the active species through the separator, or to the loss of active vanadium to a parasitic reaction. However, the CE was similar to that for CH_3CN showing the promise of DESs as potential electrolytes for future evaluation in flow batteries. Charge and discharge voltages are respectively higher and lower than the formal cell potential obtained by voltammetry. Ohmic drop in the DES results from the low conductivity of the electrolyte and the relatively large distance between the two electrodes in the H-cell. Future experiments would involve increasing the number of possible DESs for investigation in prototype flow batteries without the need of supporting electrolytes.

Acknowledgments

The authors are grateful for financial support from the High Impact Research grant (UM.C/HIR/MOHE/ENG/18) from the Ministry of Higher Education in Malaysia. MHC is grateful to Dr. Vladimir Yufit for helpful discussions regarding electrochemical measurements.

Appendix

Preliminary experiments involved verifying the experimental arrangement using results reported in the literature.[31,32] For this purpose, 0.01 M $V(acac)_3$ was dissolved in an acetonitrile (CH_3CN) solution consisting of 0.5 M $TEABF_4$ as the supporting electrolyte. Solutions were prepared and experiments carried out in an argon-filled glove box to ensure the chemicals and solutions were not exposed to environmental oxygen and water. Cyclic voltammograms at 0.1 V s^{-1} scan rate is shown for both supporting and active electrolytes in Figure A1. Two redox couples were present within the solvent's potential window (−2.5 V to 1.5 V vs. Ag/Ag^+).

Although a direct comparison between the absolute values of reduction potentials reported earlier and those in this work is difficult (owing to the different solvents used), the voltage difference between the first and second reduction peaks are very similar to those reported elsewhere[31] and therefore verifies the three-electrode set-up employed herein.

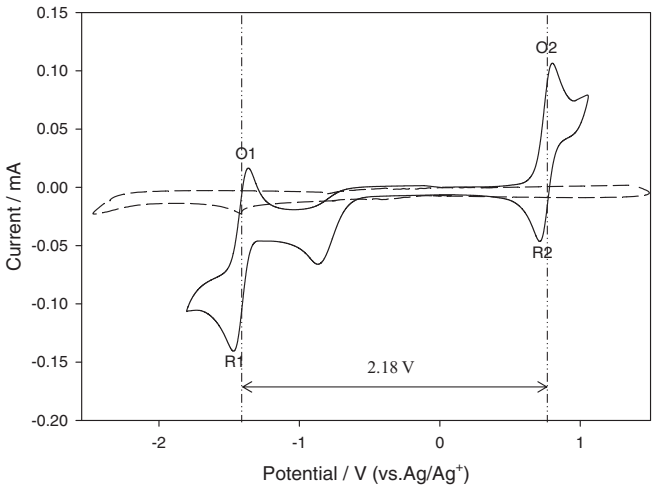

Figure A1. Cyclic voltammograms recorded at a glassy carbon electrode in 0.5 M $TEABF_4$ in CH_3CN (- - - -) and 0.01 M $V(acac)_3$ with 0.5 M $TEABF_4$ in CH_3CN (—) at 0.1 V s^{-1}. This result is similar to that reported in the literature.[31]

References

1. M. H. Chakrabarti, F. S. Mjalli, I. M. AlNashef, M. A. Hashim, M. A. Hussain, L. Bahadori, and C. T. J. Low, *Renew. Sustain. Energy Rev.*, **30**, 254 (2014).
2. M. H. Chakrabarti, R. A. W. Dryfe, and E. P. L. Roberts, *J. Chem. Soc. Pak.*, **29**, 294 (2007).
3. M. H. Chakrabarti, R. A. W. Dryfe, and E. P. L. Roberts, *Electrochim. Acta*, **52**, 2189 (2007).
4. M. H. Chakrabarti, E. P. L. Roberts, C. Bae, and M. Saleem, *Energy Conv. Manage.*, **52**, 2501 (2011).
5. M. H. Chakrabarti, S. A. Hajimolana, F. S. Mjalli, M. Saleem, and I. Mustafa, *Arab. J. Sci. Eng.*, **38**, 723 (2013).
6. G. L. Soloveichik, *Ann. Rev. Chem. Biomol. Eng.*, **2**, 503 (2011).
7. Y. Katayama, I. Konishiike, T. Miura, and T. Kishi, *J. Power Sources*, **109**, 327 (2002).
8. M. Hirao, H. Sugimoto, and H. Ohno, *J. Electrochem. Soc.*, **147**, 4168 (2000).
9. I. M. AlNashef, M. L. Leonard, M. C. Kittle, M. A. Matthews, and J. W. Weidner, *Electrochem. Solid State Let.*, **4**, D16 (2001).
10. C. A. Nkuku and R. J. Lesuer, *J. Phys. Chem. B*, **111**, 13271 (2007).
11. M. H. Chakrabarti, N. P. Brandon, F. S. Mjalli, L. Bahadori, I. M. Al Nashef, M. A. Hashim, M. A. Hussain, C. T. J. Low, and V. Yufit, *J. Solution Chem.*, **42**, 2329 (2013).
12. M. H. Chakrabarti, N. P. Brandon, M. A. Hashim, F. S. Mjalli, I. M. AlNashef, L. Bahadori, N. S. A. Manan, M. A. Hussain, and V. Yufit, *Int. J. Electrochem. Sci.*, **8**, 9652 (2013).
13. A. Boisset, S. Menne, J. Jacquemin, A. Balducci, and M. Anouti, *Phys. Chem. Chem. Phys.*, **15**, 20054 (2013).
14. C. Rub and B. Konig, *Green Chem.*, **14**, 2969 (2012).
15. A. P. Abbott, G. Capper, D. L. Davies, R. K. Rasheed, and V. Tambyrajah, *Chem. Commun.*, 70 (2003).
16. A. P. Abbott, G. Capper, K. J. McKenzie, and K. S. Ryder, *J. Electroanal. Chem.*, **599**, 288 (2007).
17. R. B. Leron and M.-H. Li, *J. Chem. Thermodyn.*, **54**, 293 (2012).
18. D. Carriazo, M. C. Serrano, M. C. Gutierrez, M. L. Ferrer, and F. del Monte, *Chem. Soc. Rev.*, **41**, 4996 (2012).
19. Q. Zhang, K. De Oliveira Vigier, S. Royer, and F. Jerome, *Chem. Soc. Rev.*, **41**, 7108 (2012).
20. M. Steichen, M. Thomassey, S. Siebentritt, and P. J. Dale, *Phys. Chem. Chem. Phys.*, **13**, 4292 (2011).
21. A. P. Abbott, K. El Ttaib, G. Frisch, K. J. McKenzie, and K. S. Ryder, *Phys. Chem. Chem. Phys*, **11**, 4269 (2009).
22. K. Pang, Y. Hou, W. Wu, W. Guo, W. Peng, and K. N. Marsh, *Green Chem.*, **14**, 2398 (2012).
23. D. Lindberg, M. de la Fuente Revenga, and M. Widersten, *J. Biotechnol.*, **147**, 169 (2010).
24. Y. Dai, J. van Spronsen, G.-J. Witkamp, R. Verpoorte, and Y. H. Choi, *Anal. Chim. Acta*, **766**, 61 (2013).
25. A. P. Abbott, T. J. Bell, S. Handa, and B. Stoddart, *Green Chem.*, **7**, 705 (2005).
26. A. P. Abbott, G. Capper, D. L. Davies, K. J. McKenzie, and S. U. Obi, *J. Chem. Eng. Data*, **51**, 1280 (2006).
27. L. Bahadori, N. S. Abdul Manan, M. H. Chakrabarti, M. A. Hashim, F. S. Mjalli, I. M. AlNashef, M. A. Hussain, and C. T. J. Low, *Phys. Chem. Chem. Phys.*, **15**, 1707 (2013).
28. D. Lloyd, T. Vainikka, and K. s. Kontturi, *Electrochim. Acta*, **100**, 18 (2013).
29. A. P. Abbott, D. Boothby, G. Capper, D. L. Davies, and R. K. Rasheed, *J. Am. Chem. Soc.*, **126**, 9142 (2004).
30. L. Bahadori, M. H. Chakrabarti, F. S. Mjalli, I. M. AlNashef, N. S. A. Manan, and M. A. Hashim, *Electrochim. Acta*, **113**, 205 (2013).
31. Q. Liu, A. E. S. Sleightholme, A. A. Shinkle, Y. Li, and L. T. Thompson, *Electrochem. Commun.*, **11**, 2312 (2009).
32. D. Zhang, Q. Liu, X. Shi, and Y. Li, *J. Power Sources*, **203**, 201 (2012).
33. L. Bahadori, M. H. Chakrabarti, M. A. Hashim, N. S. A. Manan, F. S. Mjalli, I. M. AlNashef, and N. P. Brandon, *J. Electrochem. Soc.*, **162**, H617 (2015).
34. T.-Y. Wu, S.-G. Su, Y.-C. Lin, H. P. Wang, M.-W. Lin, S.-T. Gung, and I. W. Sun, *Electrochim. Acta*, **56**, 853 (2010).
35. T.-Y. Wu, S.-G. Su, H. P. Wang, Y.-C. Lin, S.-T. Gung, M.-W. Lin, and I. W. Sun, *Electrochim. Acta*, **56**, 3209 (2011).
36. P. A. Z. Suarez, V. n. M. Selbach, J. E. L. Dullius, S. Einloft, C. M. S. Piatnicki, D. S. Azambuja, R. F. de Souza, and J. DuPont, *Electrochim. Acta*, **42**, 2533 (1997).